FEATURE ARTICLE

How Does the Solvent Control Electron Transfer? Experimental and Theoretical Studies of the Simplest Charge Transfer Reaction

Erik R. Barthel, Ignacio B. Martini, and Benjamin J. Schwartz*

Department of Chemistry and Biochemistry, University of California, Los Angeles, Los Angeles, California 90095-1569

Received: March 27, 2001; In Final Form: July 16, 2001

The standard theoretical description used to describe electron transfer is Marcus theory, which maps the polarization of the solvent surrounding the reactants onto a reaction coordinate, *q*. The questions we address in this paper are: How many and what types of solvent degrees of freedom constitute *q*? Is it appropriate to treat the solvent as a dielectric continuum? Our approach to answer these questions relies on the study of the simplest possible charge transfer systems: we choose atomic systems that have only electronic degrees of freedom so that any spectroscopic changes that occur during the course of the reaction directly reflect the motions of the surrounding solvent. Our methods for characterizing these systems consist of both molecular dynamics (MD) simulations and femtosecond pump−probe experiments. Using MD, we find that even though solvent rotational motions appear to dominate the electronic relaxation when only the solute's charge changes, the slow translational motions of the few closest solvent molecules control the solvation dynamics when realistic reactant size changes are taken into account. Moreover, we see that the linear response approximation, an assumption inherent in the use of dielectric continuum theories, fails when reactant size changes and solvent translational motions are involved. Our experimental approach focuses on the study of the charge-transfer-to-solvent (CTTS) transition of the sodium anion (Na^-). We find that the charge-transfer rate of photoexcited sodide in tetrahydrofuran is ∼3 times slower than what would be expected by assuming that dielectric solvation was the dominant driving force for electron transfer. This suggests that the slow solvent translational motions needed to accommodate the reactant size change are rate-limiting for the charge transfer process, consistent with the simulations. The electron appearance and recombination kinetics also show that even though the charge transfer rate is roughly independent of excitation energy, the distance over which the electron is ejected depends sensitively on the excitation energy. Moreover, the detached electrons recombine with their Na atom partners to regenerate the parent sodide ions on two vastly different time scales. The best way to explain the electron recombination dynamics invokes the existence of two kinds of solvated electron: geminate sodium atom contact pairs. Our molecular picture of the charge-transfer process is that low-energy excitation produces a CTTS excited-state wave function confined within the original anion solvent cavity, leading to production of a sodium atom:solvated electron contact pair that can recombine in about one picosecond. The use of high excitation energies produces CTTS excited-state wave functions with greater curvature and spatial extent, allowing the electron to localize further from the parent in a long-lived (≥200 ps) solvent-separated contact pair, or to be ejected into the solvent. Independent of the excitation energy, it is the relatively slow translational motions of first-shell solvent molecules that are responsible for the electron detachment. All the results are compared to previous experimental and theoretical work.

Introduction: the Nature of Solvent Motions in Electron Transfer Reactions

The transfer of an electron from a donor to an acceptor is one of the most fundamental transformations in chemistry and physics.[1] In the condensed phase, the dynamics of electron transfer (ET) are strongly shaped by the local environment: the importance of the solvent's influence on ET is exemplified by Marcus theory,[2,3] which is based on mapping the polarization of the medium surrounding the reactants onto a single reaction coordinate *q*. Since the number of solvent molecules surrounding the reactants is large, the fluctuations in solvent polarization around the reactants are expected to be Gaussian by the central limit theorem, giving rise to a harmonic dependence of the solvation free energy on *q*. Using this assumed parabolic form of the free energy for the solvent polarization around the donor and acceptor, Marcus theory takes advantage of simple Arrenhius activation to allow calculation of the thermally activated ET rate.[2,3] The theory has been extraordinarily successful, even for very complex ET reactions such as those that occur in biological systems.[2,4]

How do such ET reactions work on the molecular level? Figure 1 presents a cartoon snapshot of a solvent configuration

* Corresponding author. E-mail: schwartz@chem.ucla.edu.

10.1021/jp011150e CCC: $20.00
Published on Web 08/21/2001

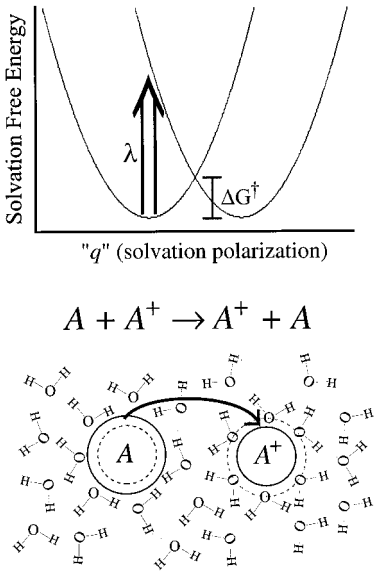

Figure 1. Bottom: a representative solvent configuration for a generic aqueous electron-transfer reaction illustrating the importance of both local solvent orientation and solute size changes. Top: two parabolas that represent the solute−solvent free energy as a function of the solvation coordinate for the system at the bottom, as typical in Marcus theory. The two curves correspond to the electron residing on the left and right species; λ and $\Delta G^{\ddagger}$ indicate the solvent reorganization energy and the activation energy, respectively. The vertical arrow on the Marcus diagram corresponds to the free energy penalty (λ) for the electron to transfer if the solvent were frozen in the configuration shown at the bottom.

for a generic aqueous electron-transfer reaction. The uncharged donor species *A* is solvated in a clathrate-like structure (nonpolar or hydrophobic solvation), with solvent H bonds directed around the solute, while the acceptor species A^+ is stably solvated in an ionic fashion. Transfer of an electron from *A* to A^+ requires significant rearrangement of the solvent molecules around each of the two reactants and, hence, costs a great deal of solvent polarization free energy. This free energy penalty for disrupting the local solvent structure, known as the solvent reorganization energy λ, is indicated by the vertical arrow on the Marcus diagram in Figure 1. By slightly distorting the solvent structure around each reactant, however, as happens naturally via thermal fluctuations, the free energy barrier for transferring an electron can be significantly lowered. On the Marcus diagram, this is represented by motion along the solvation coordinate *q*. The question we wish to address in this paper is: what are the molecular motions that constitute *q* for a typical solvent-controlled ET reaction?

Figure 1 makes it clear that part of the motions involved in *q* consist of solvent molecule reorientations: the first-shell molecules around the *A* reactant must rotate to ionically solvate the new A^+ product, while the first-shell molecules around the A^+ reactant must also rearrange to stabilize the new neutral *A* product. In addition to solvent reorientations, Figure 1 also shows that translational motions of the solvent molecules, which are necessary to accommodate the size changes of the reactants and products, will also play a significant role in the solvation coordinate *q*. In particular, as the electron is transferred away from the donor, the solvent molecules must move inward to accommodate the smaller size of the ionized product; similarly, the solvent molecules must translate away from the acceptor as it increases in size upon neutralization. When fluctuations move the solvent molecules to a configuration that would more favorably solvate the products, the probability of undergoing ET increases. With a significant enough fluctuation, the electron would be equally favorably solvated on either the donor or acceptor, indicated by the crossing point of the two Marcus curves in Figure 1. The two free energy parabolas in Figure 1 are symmetric because for this generic reaction, the reactants are identical to the products.

Although Marcus theory tells us a great deal about the energetics and kinetics of ET reactions, the theory never specifies the molecular nature of the reaction coordinate *q*. In typical applications, the Marcus theory includes components from an "inner sphere", consisting of the vibrational degrees of freedom in large molecules that drive intramolecular ET reactions, and an "outer sphere", consisting of the polarization of the surrounding solvent.[2,3] In what follows, we consider a class of ET systems whose energetics are determined entirely by the solvent, and therefore, we concentrate only on the solvent "outer sphere" motions. In applications of the Marcus theory to large molecular systems, this contribution to ET is often accounted for by modeling the solvent as a dielectric continuum. The use of dielectric continuum ideas, however, obscures the "molecularity" of the solvent by tacitly assuming that *q* consists of a linear combination of the translational, librational, and vibrational motions of many solvent molecules. For reactions like those presented in Figure 1, however, it appears that the motions of only a few of the nearest solvent molecules will be most important in accommodating the size and charge changes in a prototypical ET reaction. This idea is born out by quantum molecular dynamics (MD) simulations of the Fe^{3+}/Fe^{2+} redox couple by Bader, Chandler, and co-workers.[5] These simulations determined that even though the solvation free energy was harmonic for a range of donor/acceptor separations, the majority of the contribution came from the first and second solvent shells. A similar conclusion has been reached in work from Warshel's group, who have shown that the best results are obtained when the solvent bath is divided into "active" quantum vibronic modes that couple strongly to the reaction coordinate and passive vibronic modes that are weakly coupled to the reaction coordinate.[6] Moreover, classical MD calculations from our group, which will be discussed further below, show that the one or two solvent molecules closest to the solute provide the majority of the driving force for electronic relaxation when solute size changes are involved.[7,8] This leaves us with the questions that are the focus of this paper: in purely solvent-mediated ET reactions, what are the relative roles of solvent translational and rotational motions in driving ET? How many solvent molecular degrees of freedom are important in determining the rate of ET in such systems?

To address these questions, we need to find a system whose study can cleanly reveal the role of the solvent during ET. The ideal system would have only electronic degrees of freedom: in other words, it would consist of atomic reactants. Atomic systems have the advantage that they are simple enough to allow detailed investigation by MD. Moreover, with no internal vibrations or rotations, any spectral changes observed experimentally during the course of the reaction must result from solvent motions that affect the electronic energy of the reactants and products. Thus, the spectroscopic changes that occur as the reaction progresses in such simple systems provide a direct window on *q*, the solvent motions responsible for ET. Bimolecular reactions like the system shown in Figure 1, however, are rate-limited by diffusive encounters of the reactants. Since the members of the ensemble will undergo reaction at different times, it is impossible to extract cleanly any information about the solvent motions governing the charge transfer. Clearly, to

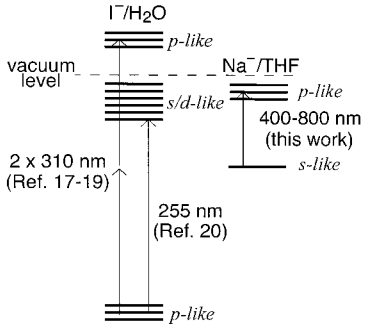

Figure 2. Simplified diagram for the CTTS energy levels of iodide (I^-) in water (left, based on refs 13 and 14) and sodide (Na^-) in THF (right). The vertical arrows represent the excitation energies used experimentally by different research groups. The absolute position of the sodide CTTS levels relative to those for iodide is estimated.

get at this type of molecular detail, it is necessary to start an entire ensemble of ET reactions simultaneously. The best way to do this is with a photoinduced ET reaction.

The reactions that satisfy all the above criteria are perhaps the simplest possible charge-transfer processes in solution: the photoinduced transfer of an electron from a monatomic anion to a cavity in the surrounding solvent. The classic examples of this type of reaction are those of the aqueous halides.[9] Gas-phase halide ions support no bound excited electronic states, but in solution, they show an intense deep-UV absorption band that has no gas-phase analogue; gas-phase studies[10] and ab initio calculations[11] show that this electronic band evolves from features present in clusters containing only a few solvent molecules. This band is commonly referred to as a charge-transfer-to-solvent (CTTS) transition;[9,12] excitation of this transition produces a neutral halogen atom and a solvated electron. Quantum molecular dynamics simulations by both Sheu and Rossky[13] and Staib and Borgis[14] have shown that CTTS excitation produces a localized state, which is bound not by the Coulomb attraction between the electron and halide nucleus but by the polarization of the solvent surrounding the anion.[15] Thus, the acronym CTTS is somewhat of a misnomer: the Franck−Condon excitation does not directly produce the product halogen atom and solvated electron. Instead, excitation places the local solvent structure around the anion donor out of equilibrium; the solvent molecules move to reestablish equilibrium, and this causes the electron to detach and become solvated in a nearby solvent cavity, which acts as the acceptor. A simplified energy diagram for the CTTS process based on these quantum simulations[13] is shown in Figure 2. Once transferred, the ejected electron remains close to its geminate (original) partner in a stable contact pair that is bound by several kT,[13,14] allowing for the possibility of a rapid back electron transfer to reform the parent anion ground state, as we will discuss further below.

The experimental technique best suited to the study of these CTTS reactions is femtosecond pump−probe spectroscopy.[16] In a pump−probe experiment, two ultrashort light pulses interact with the sample: the first (pump) pulse excites the transition to be studied, and the second (probe) pulse arrives at a later time to measure any spectral changes resulting from the excitation. The time delay between the two pulses is varied, allowing observation of the spectral dynamics of the system on the time scale(s) of the solvent motions that control ET. If the pump pulse produces a new species (such as an excited state or a photoproduct) that absorbs light at the probe wavelength, the probe transmission will decrease, resulting in a transient absorption signal. If the effect of the pump pulse is simply to remove ground-state molecules that absorb light at the probe wavelength, then the probe transmission will increase following excitation, resulting in a negative transient absorption signal due to the ground-state bleach. At some probe wavelengths, the signal will be a combination of bleaching dynamics from the loss of reactants and absorption dynamics from the appearance of intermediates or products.

Both Long et al.[17] and Gauduel and co-workers,[18] as well as others,[19] have performed femtosecond pump−probe experiments to investigate the electron detachment dynamics of aqueous halides. Because of the limitations of the ultrafast laser sources available at the time, all of these workers attempted to access the CTTS band, which lies in the deep UV ($\leq$250 nm), using multiphoton excitation, as indicated on the left half of the I^-/H_2O energy diagram in Figure 2. However, the symmetries of the states involved, together with atomic selection rules, make it unlikely that two-photon excitation could directly produce the CTTS excited state(s), which have s and/or d-like character, from the p-like halide ground state. Instead, given the energy of the photons used, the excitation in these experiments was likely to a higher-lying band of p-like states, or directly to the conduction band of water. This means that in addition to initiating the desired ET reaction from the CTTS state, the multiphoton excitation used in these experiments also produced hydrated electrons by direct ionization, masking the desired CTTS dynamics.[13,17]

Although modern laser technology recently has permitted the clean, one-photon excitation of the CTTS transition of aqueous iodide,[20] the solvent motions driving ET in this system must be inferred solely from the transient absorption dynamics of the hydrated electron. In addition, the solvent dynamics that drive ET in aqueous systems are extraordinarily fast, even by modern standards.[21,22]

In this paper, we take a somewhat different route to the study of ET dynamics by focusing on the CTTS transitions of alkali metal anions.[23,24] We will focus our attention on sodide, Na^-, due to its spectroscopic convenience: the CTTS band lies squarely in the visible range[25] and is easily accessible with the fundamental of a Ti:sapphire laser. Moreover, as we will show below, the spectra of both ET products, the neutral sodium atom[26] and the solvated electron,[27] are well-known and easily probed using modern laser systems. Although Na^- has the drawback that it cannot be prepared in water except as clusters in molecular beams,[28] this is also an advantage: the solvent motions of water are nearly too fast to be observed,[21,22] but the solvent motions that drive ET in ethers and the other nonpolar solvents in which Na^- is stable are slower and can be measured easily. Thus, the Na^- CTTS system provides a unique opportunity to capture the molecular nature of ET. The sodide/tetrahydrofuran system is the only ET reaction we are aware of for which the spectra of all the species involved in the reaction—the reactant, intermediates, and products—are known and well characterized.[23,24] And perhaps most importantly, the Na^- system has only electronic degrees of freedom so that the observed spectral changes directly reflect the motions of the solvent that drive ET: the only nuclear degrees of freedom in the system that can move are those of the solvent.

The Na^- experiments described in this paper provide a great deal of information about the time scales over which solvent motions induce charge separation, but they are not capable of directly identifying the specific solvent motions that take place on those time scales. The best way to unambiguously assign the solvent motions that are responsible for ET is to examine them via computer simulation. In a typical MD simulation, the

effects of an ET reaction are mimicked by suddenly changing the charge on a solute, which places the surrounding solvent out of equilibrium. The solvent then responds to this change by moving to stabilize the new solute; the resulting relaxation is known as solvation dynamics. The quantity usually monitored is the difference in solvation energy (the sum of all the solute−solvent interaction pair potentials) between the original solute and the newly modified solute, $\bar{U}(t) = \bar{E}_{new}(t) - \bar{E}_{orig}(t)$, where the overbar denotes a nonequilibrium ensemble average. This solvation energy gap decreases with time as the solvent moves to stabilize the new solute, a process that also destabilizes the original solute. To better compare the solvent relaxation between different systems, the solvation energy gap is often used to compute the nonequilibrium solvent response function

$$S(t) = \frac{\bar{U}(t) - \bar{U}(\infty)}{\bar{U}(0) - \bar{U}(\infty)} \quad (1)$$

which has the same dynamics as $\bar{U}(t)$ but is normalized to start at unity at time zero and decay to zero at infinite time. If the change the solute undergoes is "small", then the Onsager regression hypothesis states that the solvent motions that cause relaxation following the perturbation of the solute are the same as the solvent fluctuations present at equilibrium.[29] If the motions are indeed the same, known as the linear response (LR) limit, then the equilibrium solvent response function

$$C(t) = \frac{\langle \delta U(0) \delta U(t) \rangle}{\langle (\delta U)^2 \rangle} \quad (2)$$

where $\delta U(t) = U(t) - \langle U \rangle$ and the angled brackets denote an equilibrium ensemble average, should decay identically to $S(t)$ (eq 1).[29] Examples of both of these response functions are shown below in Figure 3. For ET reactions, the use of dielectric continuum models to approximate the solvent motions that cause relaxation implicitly assumes that the system is in the limit of LR.[30]

Most of the work on solvation dynamics has focused on describing the response to changes in solute charge distribution (dielectric solvation).[31] When only the charge of the solute changes, most of the response to accommodate the new charge involves librations (hindered rotations) of the solvent molecules; these rotational motions are present at equilibrium, and indeed, the dynamics can be understood in the context of dielectric continuum models.[31,32] Fewer studies in this field, however, have taken changes in solute size (nonpolar or mechanical solvation) into account.[33−36] In this paper, we will present simulations that explore the effects of simultaneously altering both the charge and size of a solute,[7,8] a situation designed to best approximate the changes that happen in CTTS reactions. What we will show is that large-amplitude translational solvent motions, not rotational motions, become the rate-limiting factor in solvation dynamics when the reaction involves changes in solute size. We will also show that when translational motions are a major part of the solvation coordinate, the LR approximation (which is invoked in many simulation studies as well as in dielectric continuum models) fails severely: in other words, the solvent motions present at equilibrium ($C(t)$, eq 2) are not the same solvent motions responsible for driving nonequilibrium ET reactions ($S(t)$, eq 1).

The purpose of this paper is to show that taken together, our experimental work on the CTTS reaction of Na^- and our computer simulation studies of solvation dynamics provide new insights into the nature of q, the reaction coordinate underlying solvent-mediated ET reactions. The rest of this paper is organized as follows. First, we will show how MD simulations point to a picture in which the translational motions of just the closest one or two solvent molecules play the dominant role in accommodating the new size of the reactants during ET. The fact that translational motions are rate-limiting leads to solvent relaxation that is significantly slower than that predicted using the LR approximation. Next, we discuss femtosecond experiments on the CTTS transition of Na^- in tetrahydrofuran (THF) and show that the ET reaction takes well over half a picosecond to complete. This time scale for ET is quite a bit slower than the ∼230 fs dielectric relaxation time of THF,[37] consistent with the idea that the solvent cannot be treated as a dielectric continuum and that ET is rate-limited by solvent translations. We then discuss the details of the CTTS process, including the fact that the ejected electron resides close by the parent atom in a contact pair. Finally, with all the detailed information available from both the simulations and experiments, we conclude by speculating on how this understanding affects our physical insight into the nature of ET reactions.

Simulations of Solvation Dynamics when Solutes Change Size: The Importance of Solvent Translations

As emphasized in Figure 1, for small electron donors or acceptors, the motions of solvent molecules in the vicinity of the reactants drive electron transfer in the condensed phase. The fundamental question we wish to address in this section is: What are the specific motions of the solvent involved in this class of reactions? Molecular dynamics simulations provide a unique and relatively unambiguous means of analyzing these motions separately: since the trajectory of each solvent molecule is known throughout the course of the evolving reaction, it is relatively easy to distinguish which solvent degrees of freedom contribute to the process. As mentioned above, most simulation studies of solvation dynamics have examined only dielectric relaxation: that is, they have studied the solvent motions that result when a solute undergoes a change in charge.[31] Since the electrostatic forces between the solute and solvent are long ranged, one would expect that the collective motions of many molecules will contribute to the electronic relaxation dynamics. Thus, it is not surprising that dielectric continuum ideas have been relatively successful at describing this type of solvent relaxation.[31,32]

The discussion of Figure 1 above suggests that in addition to dielectric relaxation, translational solvent motions are also important in charge transfer, even for highly charged species in polar solvents like water. This is because the transfer of an electron to ionize or neutralize a reactant produces a product with a significantly different size so that solvent molecule translation is required to accommodate the ET reaction products. Indeed, translational motions also have been shown to be important in MD simulations of charge transfer even when the solute does not explicitly undergo a change in size.[38] Moreover, for ET reactions in which the solute size does change, the energetics involved are not trivial. For example, conjugated organic molecules (like those used to probe solvation dynamics) can experience an average size increase of ∼10% upon photoexcitation,[7,39] and atomic reactants can change size by over 20% upon the addition or removal of an electron.[40] Our MD simulations show that the solvation free energy associated with size changes in this range is on the same order as that of the solvation energy accompanying the addition or removal of a fundamental unit of charge, even for charged solutes in water.[7] For solutes in less polar solvents, we expect that mechanical solvation effects will play an even more dominant role.

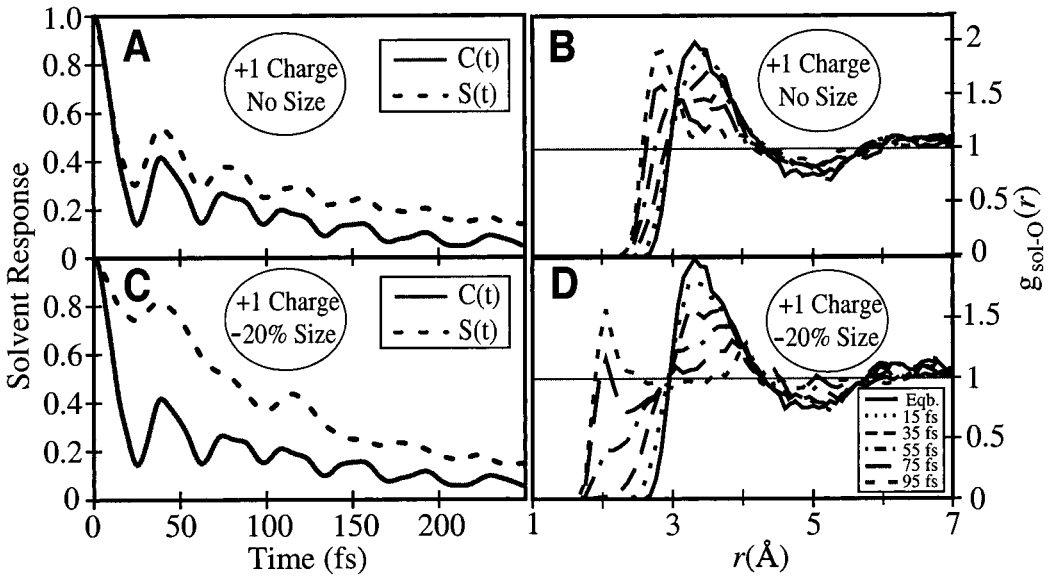

Figure 3. Simulated solvation dynamics for a Lennard−Jones solute in flexible water. Panels A and C show both the equilibrium ($C(t)$, eq 2, solid curves) and nonequilibrium ($S(t)$, eq 1, dashed curves) solvent response functions, while panels B and D show the corresponding time-dependent solute−solvent oxygen atom radial distribution functions [$g_{sol-O}(r)$]. The solid curves in panels B and D represent the equilibrium solvent structure around the solute (same in both panels), while the various dotted and dashed curves show the evolution of the solvent structure as a function of time after the solute is changed. Panels A and B show the "dielectric" case where the solute undergoes a positive change in charge with no change in size; panels C and D show the more realistic case for CTTS when the solute undergoes a positive change in charge with a simultaneous 20% size decrease.

To understand the solvation dynamics associated with solute size changes, we performed a series of MD simulations in which we changed a solute's size and/or charge and monitored the resulting response of the solvent (water). The details of the simulations are described in a previous paper.[8] Briefly, the simulations consist of several hundred water molecules (described by the Flexible SPC model[41]) and an atomic (Lennard−Jones) solute. We calculated the difference in solute−solvent interaction energy for the original solute and the newly charged/size-changed solute to compute both the equilibrium (eq 2, $C(t)$) and nonequilibrium (eq 1, $S(t)$) solvent response functions. We also monitored the (nonequilibrium) solvent structure around the solute as a function of time after the charge/size change.

Figure 3 shows the equilibrium ($C(t)$) and nonequilibrium ($S(t)$) solvent response functions following a +1 change in the charge of the solute both with (panel C) and without (panel A) an accompanying size decrease. Figure 3B,D shows how the solute−solvent radial distribution function, $g(r)$, changes with time following the change in the solute. Figure 3B shows that in the no-size-change case, the closest solvent molecules move inward (toward the solute) by roughly 10% of the solute's diameter following the appearance of charge on the solute. This is the result of the Coulombic attraction between the newly created charge on the solute and the solvent dipoles; the inward motion is often referred to as "electrostriction". The fact that the equilibrium and nonequilibrium response functions agree so well (Figure 3A) indicates that the electrostrictive translational solvent motions are similar to the solvent translations naturally present at equilibrium: the system is in the limit of linear response.

In contrast, Figure 3C shows the equilibrium and nonequilibrium solvent response functions when a +1 charge change is accompanied by a 20% decrease of the Lennard−Jones σ parameter in the solute−solvent interaction potential; this is a realistic scenario for the loss of an electron following CTTS from a solute such as iodide or sodide.[40] The figure shows that the nonequilibrium response $S(t)$ (dashed line) is nearly 1 order of magnitude slower than the equilibrium response $C(t)$ (solid line), indicating that the linear response assumption has failed. The corresponding solvent structure in Figure 3D shows that to reestablish equilibrium, the closest solvent molecules must move in by nearly ∼30% of the solute diameter: the solvent molecules must move inward ∼10% because of electrostriction and an additional ∼20% from the decrease in the solute's size. The breakdown of linear response results from the fact that solvent molecules cannot translate inward by 30% of the solute diameter at equilibrium: the repulsive forces between the solute and solvent are simply too great for the solvent to access this region with the available thermal energy. Thus, as verified by a detailed spectral density analysis,[8] different solvent motions are required to stabilize the ionic product than are available to solvate the neutral reactant at equilibrium.

Why is the solvent response so slow when the solute changes size? The simple reason is that relaxation cannot occur until after the slow, low-frequency solvent translational motions that accommodate the size decrease are complete. This is because the inward motion of the first solvent shell strongly affects the solute's energy gap by destabilizing the original solute−solvent interaction potential, so the relaxation of the energy gap is rate-limited by these inward translational motions. Our analysis of the solvent motions for the combined size-and-charge change found two remarkable features. First, we found that the bulk of the solvent response results from the motions of just the closest one or two solvent molecules.[7] This results from the steepness of the repulsive part of the solute−solvent interaction potential. For a $1/r^{12}$-type potential, if the closest solvent molecule is 10−15% closer than its neighbors, it will carry roughly 5 times more solute−solvent interaction energy than the rest of the solvent. Second, we found that at the instant the solute undergoes the size change, the closest solvent molecule is, on average, moving toward the solute only half the time.[8] The other half of the time, the closest solvent molecule is moving away from the solute. Thus, the bulk of the relaxation cannot occur until this molecule moves away from the solute, collides with the second solvent shell, and then moves back toward the solute or until another first-shell solvent molecule diffuses inward to become

the closest molecule. This explains why it takes so long to reestablish the solvent structure around the solute after it has decreased in size, as seen in Figure 3D: half the time, the closest molecules responsible for relaxation are moving the wrong direction. The resulting nonequilibrium solvent response is therefore much slower than that predicted by the equilibrium solvent dynamics.[7,8]

Given that the MD simulations predict a slow solvent response whenever translational solvent motions are involved due to solute size changes, the question is: Can this effect be observed in real (experimental) systems? The nonequilibrium solvent response of water has been measured experimentally by Fleming and co-workers using Coumarin 343, a solute which undergoes an ~8 D dipole moment change upon excitation, as a solvation probe.[21] MD simulations that accounted only for the change in charge distribution of the Coumarin solute were able to reproduce the long-time tail of the experimental solvent response, but the simulations overestimated the initial relaxation (which constitutes about half of the total solvent response) by a factor of 2.[21] We performed a simple quantum chemistry calculation on Coumarin 343 and noticed that in addition to the dipole change, the excited state is larger in size (as measured by electron density contours) than the ground state by nearly 15%.[7] When we combined a 15% size increase with the 8D dipole moment change in our own simulations using a simple L−J solute, we were able to reproduce the experimentally measured solvation dynamics at early times.[7]

In the next section, we turn to a second experimental example that supports the idea that solvent translational motions and solute size changes are important in ET reactions: the experimental study of the CTTS dynamics of the sodium anion in tetrahydrofuran. What we will show is that for this reaction, the charge-transfer time is indeed much slower than the dielectric solvation time:[37] the translational solvent motions that accommodate the large size change in this photoinduced ET reaction are not the same solvent motions which respond to the change in dipole moment of an excited dye molecule.

Alkali Metal Anions: Ideal Systems for Studying Charge-Transfer-to-Solvent

In the Introduction, we argued that the best solvent-mediated charge transfer systems to study should have only electronic degrees of freedom. In addition, a good system should be straightforward to prepare, have a spectroscopically accessible charge-transfer band, and have reactants, intermediate states, and products that are easy to characterize optically. In this section, we show that the CTTS transitions of the alkali metal anions, and that of Na^- in particular, fulfill all of these requirements.

At first, the idea of creating negatively charged alkali metal ions seems a bit counterintuitive since alkali metals are usually found in solution with a +1 valence. Over the past 30 years, however, the work of many groups, in particular that of Dye and co-workers, has established that the dissolution of alkali metals in amines and ethers leads to an equilibrium between alkali metal cations and anions (eq 3):[25]

$$2M_{(s)} \Leftrightarrow M^+ + M^- \qquad (3)$$

where M represents an alkali metal.[42] With the addition of cryptands or crown ethers, which serve as complexing agents for the alkali metal cations, the equilibrium in eq 3 can be shifted to the right, favoring formation of the anion. The effect of the complexing agents is so powerful that alkali metal anions can be produced in a variety of polar aprotic solvents, such as ethers, even when the dissolution of the metal does not occur in the absence of such agents.[25] The metal anions produced in these solutions are characterized by intense, broad, and featureless absorption spectra in the visible or near-IR.[43] These absorption spectra show all the characteristics of CTTS transitions,[9] including a linear shift of the absorption peak to the red with increasing temperature,[44] a correlation between the position of the solution absorption and that of the neutral metal, and a correlation between the position of the solution absorption and that of the well-known halide CTTS bands in different solvents. Excitation of this band produces a neutral sodium atom and a solvated electron.[45,46] For the experiments described here, we prepared the sodide solutions using an adaptation of the procedure of Dye;[47] complete details of our sample preparation have been published previously.[23,24]

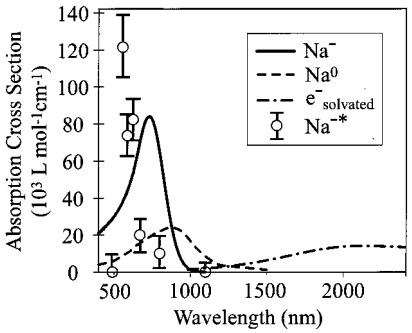

Figure 4. Absorption spectra of all the species involved in the CTTS reaction of sodide (Na^-) in THF on an absolute scale. The solid curve shows the spectrum of Na^- (this work and ref 46), the dashed curve shows the absorption spectrum of Na^0 [26, 48], the dot−dashed curve shows the absorption spectrum of the solvated electron in THF [27], and the circles show the absorption spectrum of the Na^-* excited state as determined by the "delayed ejection" model (this work); see text for details.

The Na^-/tetrahydrofuran (THF) system is particularly convenient because the spectra of both the neutral sodium species[26] and solvated electron[27] products, as well as that of sodide itself,[25] are well-known in this solvent. Figure 4 shows the absorption spectrum of Na^- in THF (solid curve), the absorption spectrum of the solvated electron in THF (dot−dashed curve), and the absorption spectrum of the species with stoichiometry Na^0 (dashed curve), which, as we argued previously (and will argue further below), is best thought of as a solvated sodium atom.[48] The circles in Figure 4 show the absorption spectrum of the excited CTTS state (Na^-*), as determined by fitting a model to the experimental pump−probe data, described further below. It is worth emphasizing that the separation of the absorption bands seen in Figure 4 allows us to probe each species, the ground-state bleach of the Na^- reactant, the absorption of the Na^-* excited intermediate, and the absorption of both the Na^0 and solvated electron products, in an essentially independent fashion.

Femtosecond Pump−Probe Experiments on Na^- in THF: The Dynamics of CTTS

Figure 5 shows the results of femtosecond experiments (circles) in which Na^- is excited at either 590 nm or near 500 nm, and the subsequent dynamics are probed at different wavelengths throughout the visible spectrum. Since the Na^- ground state absorbs strongly throughout the visible (Figure 4), the expectation is that the signal at these wavelengths should be a bleach (negative change in absorbance): the bleach should recover only after both the CTTS detachment and the back

electron transfer to reform the parent ground state Na^- have taken place. Indeed, for red probe wavelengths such as 670 or 800 nm or blue probe wavelengths such as 490 nm, the expected rapid bleach signal followed by a slower recovery is observed (Figure 5, top left and bottom right two panels). Probe wavelengths chosen between these extremes, however, show an intense transient absorption at early times, which appears to be centered in a relatively narrow spectral region near 590 nm (Figure 5, bottom left and top right panels).[23] This absorption decays within the first picosecond, leaving the negative signal characteristic of the ground-state bleach at longer times.

The fact that none of the products of the CTTS reaction are expected to absorb strongly near 590 nm and that the transiently absorbing species at 590 nm lives for such a short time suggest that this absorption is associated with the excited Na^- CTTS state (Na^{-}*).[49] Since the CTTS excited state decays due to solvent motions that cause detachment of the excited electron, the decay of the 590 nm absorption of this state provides a direct spectroscopic window into the charge-transfer process. To investigate this idea, we tested a kinetic model of the CTTS and subsequent geminate recombination process based on the quantum MD simulations both by Staib and Borgis[14] and by Sheu and Rossky,[13] who studied the related aqueous halide CTTS systems. The model assumes that once the sodide CTTS excited state is prepared, it takes time for solvent fluctuations to promote the detachment of the electron; for this reason, we call this picture the "delayed ejection" model. The model is described by the following kinetic equations:

$$Na^- \xrightarrow{h\nu} Na^-* \tag{4}$$

$$Na^-* \xrightarrow{\text{CTTS; } k_1,\, p} (Na^0 \cdot e^-)_{im} \tag{5}$$

$$Na^-* \xrightarrow{\text{CTTS; } k_1,\, 1-p} (Na^0 \cdot e^-)_{distr} \tag{6}$$

$$(Na^0 \cdot e^-)_{im} \xrightarrow{\text{recomb; } k_2} Na^- \tag{7}$$

$$(Na^0 \cdot e)_{distr} \xrightarrow{\text{recomb; diffusion; } k(E)} Na^- + Na^0 + e^-_{solvated} \tag{8}$$

The model assumes that the initially prepared CTTS excited state, Na^-* (eq 4), decays via local solvent motions with rate k_1 via detachment of the electron into multiple species. Some fraction (p) of the electrons are detached into immediate contact pairs (subscript im), in which the solvated electron resides in the same solvent cavity as the sodium atom (eq 5), while the remaining fraction ($1 - p$) localize over a distribution of distances farther from the parent atom (subscript distr, eq 6). Of those electrons that localize farther away, we expect some to be trapped metastably in what we call solvent-separated contact pairs (discussed further below), while the remainder behave simply as free solvated electrons. The fraction of electrons trapped in solvent-separated contact pairs, as well as the fraction p trapped in immediate contact pairs, will depend sensitively on the excitation energy of the pump photon. The immediate contact pairs undergo the back electron-transfer reaction (geminate recombination) with rate k_2 (eq 7), while the solvent-separated contact pairs and free electrons recombine on longer time scales with a distribution of rate constants that depends on the excitation energy, $k(E)$ (eq 8). At short times ($t \leq 10$ ps), the $k(E)$ contribution to geminate recombination from the solvent-separated contact pairs and free electrons, eq 8, is negligible. Therefore, the data in Figure 5 were fit to a model consisting solely of eqs 4−7.

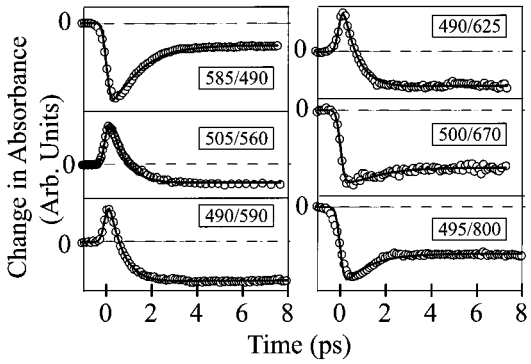

Figure 5. Femtosecond transient absorption dynamics following excitation of Na^- in THF. Top right panel: excitation at 585 nm and probing at 490 nm. The remaining panels show excitation at ~500 nm and probing (from top to bottom and left to right) at 560, 590, 625, 670, and 800 nm. Positive signals correspond to excited-state absorption, while negative signals correspond to bleaching of the ground-state Na^- absorption. The circles are the experimental data, and the solid curves are fits to the "delayed ejection" model; see text for details.

Although the model represented by eqs 4−7 assumes that immediate and solvent-separated contact pairs behave as distinct kinetic entities, we do not assume that the absorption spectra of the contact pairs are different from the sum of the separate absorptions of the Na^0 species and solvated electron, as has been proposed by others.[18] The model is limited in that it implicitly assumes that solvation dynamics do not shift the absorption spectra of any of the kinetic species; we will discuss the role of solvation in the CTTS process in more detail below. Finally, we note that the model presented above, although mathematically equivalent to the model we presented earlier,[23] reflects a new understanding of the underlying physical processes involved in CTTS based on data taken after our original paper.[50]

The solid lines in Figure 5 are a global nonlinear least-squares fit of the delayed ejection model (eqs 4−7) to the data. The best fit gives a CTTS electron-transfer time of $\tau_1 \equiv 1/k_1 = 0.7 \pm 0.1$ ps and a recombination time of $\tau_2 \equiv 1/k_2 = 1.0 \pm 0.2$ ps. For excitation at ~500 nm, we find the best-fit recombination fraction of immediate contact pairs $p = 0.25 \pm 0.1$, with the fraction increasing with increasing excitation wavelength, as discussed further below. The Na^{-*} absorption cross sections at each wavelength are also fitting parameters and are plotted as the circles in Figure 4; the estimated uncertainty in the cross sections are shown by the error bars in Figure. As is apparent, the model describes the data remarkably well, especially given the complexity of the experimental transients and the relatively small number of fitting parameters. More details of the fitting procedure are described elsewhere.[23]

In addition to probing the ground-state bleach of sodide and the CTTS excited-state absorption at visible wavelengths, we also probed the reaction products at wavelengths in the infrared. While there is a great deal of overlap between the spectra of sodide and Na^0 (Figure 4), the extinction coefficient of sodide is essentially zero for wavelengths longer than 1100 nm. Therefore, 1150 nm light makes an excellent choice for probing the Na^0 product.[51] The 1150 nm probe data are shown in Figure 6; the solid curve is a fit to the delayed ejection model using the same rate constants as those used for the visible data shown in Figure 5. As is clear from the figure, the model provides a good description of the absorption dynamics of Na^0 and, hence,

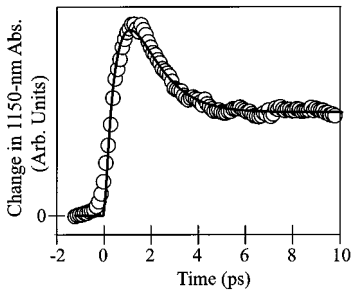

Figure 6. Femtosecond transient absorption dynamics following 615 nm excitation of Na^-/THF when probing the Na^0 product at 1150 nm. The solid curve through the data points is the fit to the "delayed ejection" model described in the text.

gives an accurate and self-consistent "zeroth order" picture of the CTTS dynamics of the sodide in the THF system.

The fact that CTTS occurs in ~700 fs and not in the ~230 fs time suggested by time-dependent Stokes shift experiments on fluorescent dyes[37] is highly suggestive of an ET reaction dominated by the translational motions of just a few solvent molecules rather than the collective motions of a dielectric continuum. This view that translational motions dominate CTTS dynamics is also supported by work on other systems. In the detachment of electrons from CTTS excitation of aqueous iodide, Bradforth and co-workers measured a ~200 fs time for appearance of the electron.[20] This value is in excellent agreement with the simulated nonequilibrium solvent response function (for the case that best mimics detachment of an electron from iodide in water) shown in Figure 3C.[8] Bradforth and co-workers also have measured the electron detachment kinetics of iodide in D_2O and find no isotope effect on the electron appearance time again consistent with the idea that solvent translations and not rotations are responsible for driving ET.[52]

Finally, it is worth noting that the appearance of the solvated electron's absorption near ~2 μm is slightly faster than the 700 fs CTTS time observed in the decay of the 590 nm Na^{-*} absorption and the 1150 nm rise of the Na^0 species.[23,24] We attribute this apparently faster rise of the electron's absorption to the diffuse nature of the electronic wave function during charge transfer. The delocalized CTTS excited-state wave function may absorb in the IR directly upon excitation, resulting in a small component of an instrument-limited absorption from the CTTS excited state. We expect that this absorption would decay faster than our time resolution due to the solvation dynamics that ultimately cause the electron to be ejected and the fact that this absorption is convoluted with the delayed ejection of the electrons on the hundreds of femtoseconds time scale. This idea of a red-shifted absorption from the newly delocalizing excited CTTS electron matches closely with the quantum molecular simulations of the CTTS process in aqueous iodide.[13] The "excess" near-IR absorption observed at early times in femtosecond experiments studying the CTTS dynamics of iodide[53] also may result from this type of solvent-induced electronic delocalization of the newly excited CTTS electron.

Overall, the minor difference between the appearance times of the electron and Na^0 products, as well as the other small differences between the fits and the data seen in Figure 5, can be explained by spectral evolution of the kinetic species that is not accounted for in the delayed ejection model. For example, Ruhman and co-workers recently have measured the polarized bleaching dynamics of Na^- in THF and have concluded that the ground state absorption is inhomogeneously broadened.[54] This observation suggests that there could be spectral diffusion in the ground-state bleach that is not accounted for in the delayed

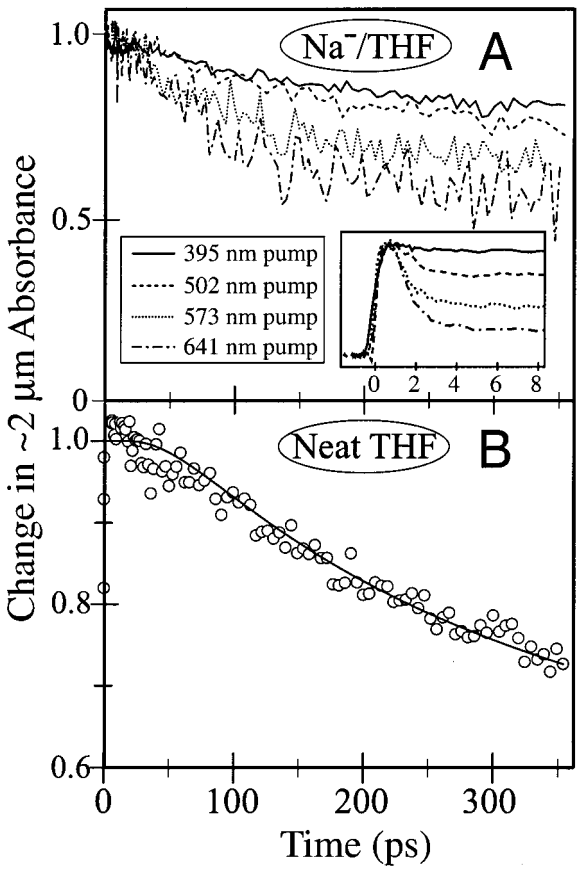

Figure 7. Femtosecond transient absorption dynamics, probed at ~2 μm, of solvated electrons in THF that were produced in two different ways: (A) Following excitation of Na^- in THF using different pump wavelengths (from top to bottom): 395, 502, 573, and 640 nm. The transients in the main figure are normalized to the same absorbance at 8 ps; the inset shows the same data on a shorter time scale normalized to the maximum transient absorption. (B) Following multiphoton ionization of THF at 395 nm. The solid line is a fit to a diffusion model as described in the text. Note that the vertical axis in this panel is expanded for clarity.

ejection model.[55] The experiments by Ruhman and co-workers are performed with ~30 fs time resolution, allowing observation of solvent dynamics that shift the spectra of all the species involved in the reaction. This gives rise to a complex spectral evolution that cannot be completely captured with simple kinetic models of the type presented here.[54] We expect that the ~700 fs ejection time obtained from the delayed ejection model represents a mixture of solvation and detachment processes that are required for the CTTS reaction to reach completion.

Recombination Dynamics Following CTTS: The Nature of Contact Pairs

The delayed ejection model implies that a significant fraction of the contact pairs recombine in ≤1 ps, presumably the result of a direct nonadiabatic transition resulting from overlap of the relatively diffuse solvated electron's wave function with that of the nearby sodium atom. What happens to those electrons that do not recombine directly? Figure 7A shows the long-time transient absorption that results from probing the solvated electron in THF at 2 μm following excitation of the CTTS band of sodide at a variety of wavelengths: 395, 502, 573, and 640 nm, from top to bottom. To better compare the dynamics after the fast recombination, the transients in the main part of the figure are normalized at 8 ps delay, while the inset shows the same dynamics from time zero to 8 ps, normalized to the

maximum of the transient absorption signal. The figure makes it clear that recombination takes place on multiple time scales: not only is there significant recombination in the first few picoseconds after excitation, but there is also additional recombination that takes place over a time of hundreds of picoseconds.[24] Moreover, there is a significant excitation wavelength dependence of the relative amplitude of the two recombination processes. At short times ($t \leq 10$ ps), fits to the delayed ejection model give immediate pair recombination fractions (p) ranging from $\leq 10\%$ for 395 nm excitation to $\geq 90\%$ for 800 nm excitation, with a recombination time of ~ 1 ps for all excitation wavelengths.[24] At longer times, however, we need some mechanism to account for the recombination that takes place on the hundreds-of-picoseconds time scale, the process-(es) represented by the excitation energy-dependent rate constant-(s) $k(E)$ in eq 8.

One possibility to consider is that the $1 - p$ fraction of electrons that do not recombine at early times are "free" solvated electrons and that the long-time recombination results from the diffusion of these electrons through the solvent as they search for their geminate partners. The recombination dynamics that result from diffusive motion have already been explored in detail, especially in the radiation chemistry literature.[56,57] In a typical diffusion model, the electron and its geminate partner undergo a random walk. If the two species diffuse to within a certain reaction distance of one another, they are assumed to recombine with unit probability. Using these ideas, one can construct expressions for the time-dependent survival probability of an electron once it detaches from its parent.[24,56] The functional form of these expressions depends on the probability distribution of the initial distance that the electron starts from its partner, which is referred to as the "thermalization length". For a given distribution of ejection distances, the relevant fitting parameters are the average thermalization length and the reaction distance between the electron and its geminate partner.

We made an extensive study of the recombination dynamics of electrons produced by multiphoton ionization of neat THF and found that the diffusion model describes the data quite well, as shown in Figure 7B.[24] With ~ 4.5 eV of excess energy, Figure 7B shows that electrons ejected from THF take several hundred picoseconds to recombine with their geminate partners, which gives an average distance for electron ejection of ~ 40 Å and a recombination distance of ~ 10 Å. The fact that it takes ~ 4.5 eV of excess energy to eject an electron as far as 40 Å from its parent is consistent with previous studies of electron ejection via multiphoton ionization in other solvents.[58]

We also attempted to apply this type of diffusion model[24,56] to the long-time Na^- CTTS transients (Figure 7A), which look quite similar to the transients obtained for multiphoton ionization of the THF solvent (Figure 7B). The values we obtained when attempting to fit the diffusion model to the Na^- transients, however, are highly unphysical: in order to reproduce the observed transients, the electron would have to be ejected over 55 Å from its parent (using a ≤ 3 eV photon!) and would have to undergo recombination while still 45 Å away from the Na atom. Clearly, diffusion does not provide a satisfactory description of the long-time recombination behavior of solvated electrons produced by the CTTS transition of sodide.

Given the success of diffusion-based models for the multiphoton ionization of THF, how can we rationalize their failure to describe the long-time behavior of CTTS electrons from sodide? A cartoon summarizing our picture of the Na^- ejection and recombination processes is shown in Figure 8. Upon photoexcitation of Na^- to the CTTS excited state, we expect

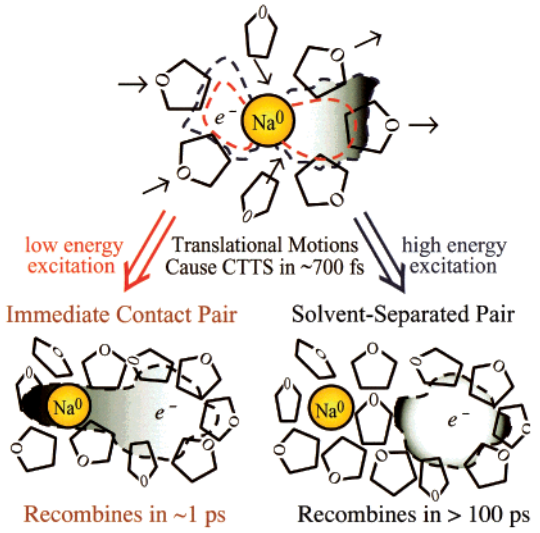

Figure 8. Schematic representation of the molecular motions involved in CTTS. The solvent shell around the ground state sodium anion is relatively far away because the excess charge of the anion is only loosely held. The upper part of the figure depicts what happens immediately following excitation. At low excitation energies, the excited state wave function spans only the region inside the first solvent shell (red wave function contour). Higher excitation energies produce excited-state wave functions with more curvature; these wave functions can extend past the first solvent shell (blue wave function contour). For either type of excitation, translational solvent motions cause detachment of the excited electron after ~ 700 fs. For low energy excitation, the electron is ejected nearby the sodium parent, resulting in an immediate contact pair that undergoes recombination in under 1 ps (lower left). Higher-energy excitation produces some probability that the electron localizes farther from the parent, leading either to a stable solvent-separated contact pair that does not recombine for hundreds of ps (lower right) or to a free solvated electron and sodium atom (not shown).

solvent motions to drive the electron detachment and cause the electron to localize near the Na^0 partner. At low excitation energies, the excited CTTS wave function is largely confined to the parent solvent cavity so that the electron will be ejected very close to the sodium atom. This localized ejection produces what we call an "immediate" contact pair, which is characterized by significant overlap of the electron's wave function with that of the sodium atom. Because of the overlap, recombination can occur by a direct nonadiabatic transition within 1 ps. In contrast, the CTTS wave functions produced at higher excitation energies have more curvature and a larger spatial extent. This greater spatial extent leads to the possibility that a significant number of electrons can detach one or more solvent shells away from their sodium partners.[59] The overlap of the wave function for these electrons, which reside at least one solvent shell from their Na atom partners, with that of the sodide ground state will be essentially zero. For those electrons that localize only one solvent shell away, the surrounding solvent molecules arrange to simultaneously stabilize both the electron and sodium atom products. This leads to a large free energy barrier to recombination: there has to be a significant fluctuation which breaks this local solvent structure and allows some direct wave function overlap before recombination can occur.[60] Evidently, these fluctuations occur relatively infrequently in THF, taking place on the hundreds-of-picoseconds time scale. Figure 8 also illustrates why the electron formation time, which is rate-limited by the translational motions of the nearest solvent molecules, is roughly independent of the excitation energy,[61] but the recombination fraction is highly

sensitive to the excitation energy because of the spatial extent of the excited-state wave function. The delayed ejection model presented in eqs 4−8 incorporates the essence of all of these ideas.

Although the idea of forming stable contact pairs is consistent with previous simulation[13,14] and experimental[20] work done on the aqueous halides, we expect that the details of the solvent motions following CTTS excitation of Na^- in THF will be different from those in the aqueous halides. Because of the s-like symmetry of the Na^- ground state,[25,62] we expect the CTTS excited states to have p-like character (Figures 2 and 8). This leads us to anticipate that the solvent motions that contribute the most to the detachment of the electron from the CTTS state will be those of THF molecules translating in toward the angular node of the p-like CTTS wave function.[63] It is this "pinching" of the wave function that forces the excess electron to localize into a contact pair, as illustrated in Figure 8. We hope to provide verification of this picture via quantum nonadiabatic simulations of the CTTS dynamics of Na^- that are presently underway in our group.

Contact Pairs: A Universal Product for CTTS

It is clear from both simulations[13,14] and experiments[20,23,24,53] that contact pairs play an important role following electron ejection via CTTS. The stability of solvent-separated contact pairs in CTTS systems tells us that the solvent structure around the pair is also stable: there is a significant barrier to destroy this structure to allow recombination. Does this idea of a contact pair hold for other CTTS systems? Recently, there have been several examples in the literature that show how recombination behavior is dependent on the local solvent structure around the solute. Bradforth and co-workers have made considerable progress in exploring the single-photon excitation of the iodide CTTS transition; this is shown as the single photon process on the right half of the I^-/H_2O energy diagram shown in Figure 2.[20] Bradforth's group also has compared the localization and recombination dynamics of electrons produced both from the CTTS transition of I^- and from the multiphoton ionization of neat water.[53] The picture that has emerged from their work is that the initial electron localization occurs on a ~200 fs time scale for both detachment processes, while the geminate recombination dynamics differ greatly between CTTS and direct photoejection. In particular, it was determined that standard diffusive models cannot describe the recombination dynamics following CTTS. Instead, the existence of a contact pair, which is consistent with both the simulation and experimental results presented above, must be invoked to explain the data.[20,53]

The importance of solvent-stabilized geminate ion pairs also fits with studies of the photoionization of indole in water by Kohler and co-workers.[64] These researchers found no measurable geminate recombination of the hydrated electron with the indole radical cation for hundreds of picoseconds following photoionization. This lack of recombination can be attributed to the high stability of the indole cation:solvated electon ion pair in polar solvents such as water. In order for recombination to take place, the solvent must undergo a fluctuation significant enough to disrupt the highly favorable ionic solvation shells around both the radical cation and the solvated electron: in the language of Marcus theory, we would say that this back ET reaction lies in the inverted regime.

All of this provides an appealing way to rationalize the observed recombination behavior not only in our studies on Na^-, but also in the related work on iodide and indole. The idea is simply that the more favorably solvated the contact pair is, the less the recombination will be. For example, if the fast recombination of the immediate contact pairs in the Na^-/THF system is ignored, we observe a much slower recombination rate for solvent-separated contact pairs following CTTS detachment of Na^- in THF (hundreds of ps) than for I^- in water (tens of ps). For the iodide case, the contact pair consists of a hydrophilic solvated electron and a nonpolar, hydrophobic iodine atom. Since the iodine atom is expected to be more poorly solvated in water than the sodium atom in THF, the iodine:electron contact pair in water is less stable and recombines more quickly than the sodium:electron contact pair in THF. The recombination rate is even slower (essentially unobservable) for indole cation:electron contact pairs in water because there is an enormous barrier to breaking up the solvent structure around two ions in a highly polar medium like water.

Our picture of immediate and stable solvent-separated contact pairs is also supported by work that is presently in progress in our group. We recently have found that the long-time recombination of solvent-separated contact pairs produced via CTTS excitation of Na^- is highly solvent-dependent: the long-time recombination is relatively fast (tens of picoseconds) in low-polarity solvents such as diethyl ether.[65] This fits perfectly with our expectation of producing a more stable solvent-separated contact pair in more polar solvents. We also have used a sequence of three femtosecond laser pulses to manipulate the distance between the electron and the Na atom throughout the entire CTTS process.[66] In these experiments, the first pulse initiates CTTS detachment of the electron from Na^-; selecting the wavelength of this first pulse allows us to control the way in which the electron is ejected. The second pulse then excites the detached electron near its absorption maximum at 2 μm into a highly delocalized, plane-wave-like state, and the third pulse monitors the resulting dynamics. The results of these experiments support the idea of two different contact pairs because the effect of the second excitation pulse is different when applied at early times (exciting predominantly immediate contact pairs) or at later times (when only solvent-separated contact pairs or free electrons remain to be excited). We find that application of the second pulse shuts off the recombination of immediate contact pairs, a result similar to that in recent work by Barbara and co-workers on the multiphoton ionization of water.[67] Excitation of the electrons in solvent-separated contact pairs, however, can promote recombination because the expansion of the electronic wave function actually improves the overlap with the geminate sodium atom. We also find that recombination is still promoted even if the electron re-excitation pulse is applied tens of picoseconds after CTTS detachment, verifying that the electrons in the solvent-separated pairs remain adjacent to their sodium atom geminate partners and do not diffuse away.[66] Finally, the fact that a single laser pulse can promote the recombination of solvent-separated contact pairs also provides a strong argument that the atomic product of the CTTS reaction is best thought of as a solvated sodium atom.[48] It is unlikely that a single laser pulse could promote the three-body recombination of two solvated electrons and a sodium cation if the second 3s electron had detached from the sodium atom product to form a sodium cation:solvated electron contact pair. The details of all this work will be presented in forthcoming publications.[65,66]

Marcus Theory and Molecularity in CTTS

In this paper, we have argued that charge-transfer-to-solvent reactions of monatomic anions serve as paradigms for solvent-

mediated electron-transfer reactions because of their relative simplicity. This simplicity allows for unprecedented detail in analyzing the effects of solvent motions on ET reactions. The basic picture of the charge ejection and recombination processes in CTTS reactions presented in Figure 8 argues that the molecular nature of the solvent is paramount in understanding how solvent motions control electron transfer. The question we consider to close this article is: How does this picture mesh with the ideas of Marcus theory?

Marcus theory describes the solute−solvent free energy in terms of a generalized reaction coordinate q (Figure 1). Because single molecule translational motions are important, it might be tempting to define q simply as the separation between the solute and the closest solvent molecule. However, this approach has several drawbacks. For example, the identity of the "closest" solvent molecule is likely to change several times over the course of an ET reaction, making any simple identification of q quite difficult. As appealing as a single-molecule picture would be, it is clear that the reaction coordinate coupled to CTTS dynamics will still require some type of statistical description. On the other hand, with only one or perhaps a few translational degrees of freedom in q, it is difficult to see how there can be a sufficient range of fluctuations to produce the Gaussian statistics required by Marcus theory to ensure that the free energy surfaces are parabolic. One method that might provide a natural Marcus description of CTTS would be to treat the closest one or two solvent molecules as vibrations of the solute (part of an "inner sphere") in much the same manner as that done for the ET reactions in mixed-metal inorganic coordination complexes.[1] Finally, and perhaps most important, the solvent response for the translational motions of the closest molecules is highly nonlinear.[8] Thus, even if the solute−solvent free energy surfaces are harmonic at equilibrium,[5] there is no reason to expect that the equilibrium solvent fluctuations will provide a good description of the nonequilibrium changes that take place during electron transfer. Our hope is that the unprecedented detail offered by the alkali metal anion CTTS systems will allow us to address all of these issues, ultimately making a connection between the dynamics of individual solvent molecules and Marcus theory.

Acknowledgment. This work was supported by the National Science Foundation under CAREER Award CHE-9733218. B.J.S. is an Alfred P. Sloan Foundation Research Fellow, a Cottrell Scholar of Research Corporation, and a Camille Dreyfus Teacher-Scholar. We thank Peter Rossky for a critical reading of the manuscript.

References and Notes

(1) For a recent review, see: Barbara, P. F.; Meyer, T. J.; Ratner, M. A. *J. Phys. Chem.* **1996**, *100*, 13148.

(2) Marcus, R. A.; Sutin, N. *Biochim. Biophys. Acta* **1985**, *811*, 265.

(3) Marcus, R. A. *J. Chem. Phys.* **1956**, *24*, 966. Marcus, R. A. *Annu. Rev. Phys. Chem.* **1964**, *15*, 155.

(4) See, e.g, Closs, G.; Miller, J. R. *Science*, **1988**, *240*, 440. DeVault, D. *Quantum Mechanical Tunneling in Biological Systems*; Cambridge University Press: Cambridge, 1984.

(5) Kuharski, R. A.; Bader, J. S.; Chandler, D.; Sprik, M.; Klein, M. L.; Impey, R. W. *J. Chem. Phys.* **1988**, *89*, 3248. Bader, J. S.; Chandler, D *J. Phys. Chem.* **1992**, 96, 6423.

(6) Jen, C. F.; Warshel, A. *J. Phys. Chem. A* **1999**, *103*, 11378.

(7) Tran, V.; Schwartz, B. J. *J. Phys. Chem. B* **1999**, *103*, 5570.

(8) Aherne, D.; Tran, V.; Schwartz, B. J. *J. Phys. Chem. B* **2000**, *104*, 5382.

(9) For a review of CTTS phenomena, see Blandamer, M. J.; Fox, M. F. *Chem. Rev.* **1970**, *70*, 59.

(10) See, e,g, Sexner, D.; Dessent, C. E. H.; Johnson, M. A. *J. Chem. Phys.* **1996**, *105*, 7231. Lehr. L.; Zanni, M. T.; Frischkorn, C.; Weinkauf, R.; Neumark, D. M. *Science* **1999**, *284*, 635.

(11) Combariza, J. E.; Kestner, N. R.; Jortner, J. *J. Chem. Phys.* **1994**, *101*, 2851.

(12) See, e.g., Jortner, J.; Ottolenghi, M.; Stein, G. *J. Phys. Chem.* **1964**, *68*, 247. Grossweiner, L. I.; Matheson, *J. Phys. Chem.* **1957**, *61*, 1089.

(13) Sheu, W.-S.; Rossky, P. J. *Chem. Phys. Lett.* **1993**, *202*, 186; **1993**, *213*, 233; *J. Phys. Chem.* **1996**, *100*, 1295. Sheu, W.-S.; Rossky, P. J.; *J. Am. Chem. Soc.* **1993**, *115*, 7729.

(14) Staib, A.; Borgis, D. *J. Chem. Phys.* **1995**, *103*, 2642. Borgis, D.; Staib, A. *Chem. Phys. Lett.* **1994**, *230*, 405. Staib, A.; Borgis, D. *J. Chem. Phys.* **1996**, *104*, 9027; *ibid.* **1996**, *104*, 4776. Borgis, D.; Staib, A. *Condens. Matt.* **1996**, *8*, 9389.

(15) Chen, H. Y.; Sheu, W.-S. *J. Am. Chem. Soc.* **2000**, *122*, 7534.

(16) Fleming, G. R. *Chemical Applications of Ultrafast Spectroscopy*; Oxford University Press: New York, 1986.

(17) Long, F. H.; Shi, X.; Lu, H.; Eisenthal, K. B. *J. Phys. Chem.* **1994**, *98*, 7252. Long, F. H.; Lu, H.; Shi, X.; Eisenthal, K. B. *Chem. Phys. Lett.* **1990**, *169*, 165. Long, F. H.; Lu, H.; Eisenthal, K. B. *J. Chem. Phys.* **1989**, *91*, 4413.

(18) Gelabert, H.; Gauduel, Y. *J. Phys. Chem.* **1996**, *100*, 13993. Gauduel, Y.; Gelabert, H.; Ashokkumar, M. *Chem. Phys.* **1995**, *197*, 167. Gauduel, Y.; Pommeret, S.; Migus, A.; Yamada, N.; Antonetti, A. *J. Opt. Soc. Am. B* **1990**, *7*, 1528.

(19) Assel, M.; Laenen, R.; Laubereau, A. *Chem. Phys. Lett.* **1998**, *289*, 267.

(20) Kloepfer, J. A.; Vilchiz, V. H.; Lenchenkov, V. H.; Bradforth, S. E. *Chem. Phys. Lett.* **1998**, *298*, 120. Kloepfer, J. A.; Vilchiz, V. H.; Lenchenkov, V. A.; Germaine, A. C.; Bradforth, S. E. *J. Chem. Phys.* **2000**, *113*, 6288.

(21) Jimenez, R.; Fleming, G. R.; Kumar, P. V.; Maroncelli, M. *Nature* **1994**, 369, 471.

(22) See, e.g, Zolotov, B.; Gan, A.; Fainberg, B. D.; Huppert, D. *J. Lumin.* **1997**, *72*, 842. Zolotov, B.; Gan, A.; Fainberg, B. D.; Huppert, D. *Chem. Phys. Lett.* **1997**, *265*, 418. Winkler, K.; Lindner, J.; Bursing, H.; Vohringer, P. *J. Chem. Phys.* **2000**, *113*, 4674. Castner, E. W.; Chang, Y. J.; Chu, Y. C.; Walrafen, G. E. *J. Chem. Phys.* **1995**, *102*, 653.

(23) Barthel, E. R.; Martini, I. B.; Schwartz, B. J. *J. Chem. Phys.* **2000**, *112*, 9433.

(24) Martini, I. B.; Barthel, E. R.; Schwartz, B. J. *J. Chem. Phys.* **2000**, *113*, 11245.

(25) For reviews on alkali metal anion solutions, see: Dye, J. L. *J. Phys. IV* **1992**, *1*, 259. Dye, J. L. *Prog. Inorg. Chem.* **1984**, *32*, 327. Dye, J. L. *J. Chem. Educ.* **1977**, *6*, 332.

(26) The absorption spectrum of the Na^0 species was provided by John Miller. See also: Piotrowiak, P.; Miller, J. R. *J. Am. Chem. Soc.* **1991**, *113*, 5086. Bockrath, B.; Dorfman, L. M. *J. Phys. Chem.* **1975**, *79*, 1509; **1973**, *77*, 1002.

(27) Dorfman, L. M.; Jou, F. Y.; Wageman, R. *Ber. Bunsen-Ges. Phys. Chem.* **1971**, *75*, 681. Jou, F. Y.; Freeman, G. R. *Can. J. Phys.* **1976**, *54*, 3693.

(28) Takasu, R.; Ito, H.; Nishikawa, K.; Hashimoto, K.; Okuda, R.; Fuke, K. *J. Elec. Spec. Relat. Phenom.* **2000**, *106*, 127. Takasu, R.; Misaizu, F.; Hashimoto, K.; Fuke, K. *J. Phys. Chem. A* **1997**, *101*, 3078. Hashimoto, K.; Kamimoto, T.; Fuke, K. *Chem. Phys. Lett.* **1997**, *266*, 7.

(29) Chandler, D. *Introduction to Modern Statistical Mechanics*; Oxford University Press: New York, 1987.

(30) See, e.g., Georgievskii, Y.; Hsu, C.-P.; Marcus, R. A. *J. Chem. Phys.* **1999**, *110*, 5307.

(31) For review articles, see: Rossky, P. J.; Simon, J. D. *Nature* **1994**, *370*, 263. Maroncelli, M. *J. Mol. Liq.* **1993**, *57*, 1. Cho, M.; Fleming, G. R. *Annu. Rev. Phys. Chem.* **1996**, *47*, 109. Maroncelli, M.; MacInnis, J.; Fleming, G. R. *Science* **1989**, *243*, 1674.

(32) See, e.g., Song, X. Y.; Chandler, D.; *J. Chem. Phys.* **1998**, *108*, 2594. Hsu, C.-P.; Song, X. Y.; Marcus, R. A. *J. Phys. Chem. B* **1997**, *101*, 2456. Ravichandran, S.; Roy, S.; Bagchi, B. *J. Phys. Chem.* **1995**, *99*, 2489. Calef, D. F.; Wolynes, P. G. *J. Phys. Chem.* **1983**, *87*, 3387;.

(33) For simulation studies on solvation following the photoexcitation and size change of the hydrated electron, see: Schwartz, B. J.; Rossky, P. J. *J. Mol. Liq.* **1995**, *65*−*6*, 23. Schwartz, B. J.; Rossky, P. J. *J. Chem. Phys.* **1996**, *105*, 6997.

(34) Other simulations involving solvation of a solute size change include: Ando, K.; Kato, S. *J. Chem. Phys.* **1991**, *95*, 5966. Herman, M. F.; Berne, B. J. *J. Chem. Phys.* **1983**, *78*, 4103. Yamaguchi, T.; Kimura, T.; Hirota, N. *J. Chem. Phys.* **1999**, *111*, 4169. Stephens, M. D.; Saven, J. G.; Skinner, J. L. *J. Chem. Phys.* **1997**, *106*, 2129. Phelps, D.; Weaver, M. J.; Ladanyi, B. M. *Chem. Phys.* **1993**, *176*, 575.

(35) For a theoretical analysis of nonpolar solvation based on instantaneous normal modes, see: Ladanyi, B. M.; Stratt, R. M. *J. Phys. Chem.* **1996**, *100*, 1266. A theoretical analysis of nonpolar solvation in terms of viscoelastic continuum theory can be found in: Berg, M. *J. Phys. Chem. A* **1998**, *102*, 17.

(36) For experimental work on nonpolar solvation, see, e.g.: Ma, J.; Vanden Bout, D.; Berg, M. *J. Chem. Phys.* **1995**, *103*, 9146. Wendt, H.; Richert, R. *J. Phys. Chem. A* **1998**, *102*, 5775.

(37) The experimentally measured solvent response functions of THF and many other liquids are tabulated in: Reynolds, L.; Gardecki, J. A.; Frankland, S. J. V.; Horng, M. L.; Maroncelli, M. *J. Phys. Chem.* **1996**, *100*, 10337.

(38) Vath, P.; Zimmt, M. B.; Matyushov, D. V.; Voth, G. A. *J. Phys. Chem. B* **1999**, *103*, 9130.

(39) See, e.g., Nowak, R.; Bernstein, E. R. *J. Phys. Chem*. **1987**, *86*, 4783 as well as ref 36.

(40) The fact that atomic species change undergo size changes of this magnitude when changing their oxidation state is obvious from standard tables of ionic and van der Waals radii. See, for example: Huheey, J. E. *Inorganic Chemistry*, 3rd ed.; Harper & Row: New York, 1983.

(41) Toukan, K.; Rahman, A. *Phys. Rev. B* **1985**, *31*, 2643.

(42) The actual equilibria are somewhat more complex than depicted in eq 3 and involve solvated electrons as well as metal cations and anions; see ref 25 for details.

(43) See, e.g.: Matalon, S.; Golden, S.; Ottolenghi, M. *J. Phys. Chem.* **1969**, *73*, 3098. Lok, M. T.; Tehan, F. J.; Dye, J. L. *J. Phys. Chem.* **1972**, *76*, 2975.

(44) Lok, M. T.; Tehan, F. J.; Dye, J. L. *J. Phys. Chem.* **1972,** *76*, 2975.

(45) Early flash photolysis work on alkali metal anions can be found in: Huppert, D.; Rentzepis, P. M.; Struve, W. S. *J. Phys. Chem.* **1975**, *79*, 2850. Huppert, D.; Rentzepis, P. M. *J. Phys. Chem.* **1976**, *64*, 191. Kloosterboer, J. G.; Giling, L. J.; Rettschnick, R. P. H.; Van Voorst, J. D. W. *Chem. Phys. Lett.* **1971**, *8*, 462.

(46) Seddon, W. A.; Fletcher, J. W. *J. Phys. Chem.* **1980**, *84*, 1104.

(47) Dye, J. L. *J. Phys. Chem.* **1980**, *84*, 1084.

(48) There is some difference of opinion in the literature about how to identify the neutral alkali metal species in solution. One possibility is that this species is an ion pair between a solvated electron and an alkali metal cation. In refs 23 and 24, however, we have argued that the transient spectroscopy of these systems show no dynamics that could be associated with a second electron detaching from the metal anion, identifying the neutral species as a genuine solvated metal atom.

(49) We attribute this ~590 nm transient feature to absorption of the Na^0 core following excitation of one of the Na^- 3s electrons into the CTTS excited state. The core atom is shielded from the solvent by the excited, Rydberg-like CTTS electron and, thus, has a 590 nm absorption similar to that in the gas phase (the famous Na "D" line). It is not until the CTTS electron detaches and the atom is solvated that the spectrum becomes that shown by the dashed curve in Figure 4.

(50) Equations 4−8 are different than the older version of the delayed ejection model presented in ref 23. In the older version of the model, there was only one species, an immediate contact pair, formed by the CTTS detachment process. The longer-time data presented in Figure 7, however, combined with the results of solvent-dependent experiments in ref 65 and multiple-pulse sequence experiments in ref 66, justify the direct formation of solvent-separated contact pairs and free electrons from the initially prepared excited state, as reflected in Figure 8. Equations 4−7, however, are mathematically equivalent at short times to the older model in ref 23 when k_2 of the old model is replaced by $k_2{*}p$ in the new model.

(51) As shown in Figure 4, the absorption of the solvated electron in THF is fairly appreciable at 1150 nm, ~$^1/_3$ that of Na^0. However, the appearance and recombination dynamics of the electron are nearly identical to those of Na^0. Even if the known cross-section of the solvated electron is not included in the delayed ejection model, the omission does not alter the quality of the fit seen in Figure 6.

(52) Bradforth, S. E. Private communication, 2001.

(53) Vilchiz, V. H.; Kloepfer, J. A.; Germaine, A. C.; Lenchenkov, V. A.; Bradforth, S. E. *J. Phys. Chem. A* **2001**, *105*, 1711.

(54) Wang, Z.; Shoshana, O.; Ruhman, S. *Proceedings of the 12th International Conference on Ultrafast Phenomena*; Springer Series in Chemical Physics 66; Springer-Verlag: Berlin, 2001. Wang, Z.; Shoshana, O.; Ruhman, S. *J. Chem. Phys.*, submitted.

(55) Polarized hole-burning provides the possibility of spectrally separating multiple electronic transitions with orthogonally oriented transition dipoles, as has been done experimentally for the permanganate anion (Yu, J. W.; Berg, M. *J. Phys. Chem.* **1993**, *97*, 1758) and both experimentally and in quantum MD simulations for the hydrated electron (Schwartz, B. J.; Rossky, P. J. *Phys. Rev. Lett.* **1994**, *72*, 3282. Reid, P. J.; Silva, C.; Walhout, P. K.; Barbara, P. F. *Chem. Phys. Lett.* **1994**, *228*, 658).

(56) For the theoretical treatment of diffusive recombination of solvated electrons generated from multiphoton ionization or absorption of high energy radiation, see, e.g.: Green, N. J. B. *Chem. Phys. Lett.* **1984**, *107*, 485. Clifford, P.; Green, N. J. B.; Pilling, M. J. *J. Phys. Chem*. **1982**, *86*, 1318. Goulet, T.; Jay-Gerin, J.-P. *J. Chem. Phys*. **1992**, *96*, 5076. Green, N. J. B.; Pilling, M. J.; Pimblott, S. M.; Clifford, P. *J. Phys. Chem.* **1990**, *94*, 251.

(57) For recent experimental studies of solvated electrons produced via multiphoton ionization, see: Thomsen, C. L.; Madsen, D.; Keiding, S. R.; Thøgersen, J. *J. Chem. Phys.* **1999**, *110*, 3453, and references therein.

(58) Crowell, R. A.; Bartels, D. M.; *J. Phys. Chem.* **1996**, *100*, 17940.

(59) Given the evidence of Ruhman and co-workers in ref 54 that the absorption spectrum of Na^- is inhomogeneously broadened, the band likely consists of 3 quasi-degenerate s → p transitions whose energy is split by the local asymmetry of the solvent and possibly an additional transition on the blue side, corresponding to detachment of the electron directly into the solvent continuum. Tuning the Na^- excitation wavelength changes the relative fraction of each of these transitions that is excited, thus changing the relative fraction of electrons that localize nearby or far from their parent sodium atoms.

(60) It is possible to estimate the height of this barrier using theory, as in the fourth article in ref 14. However, at this time, there is not sufficient experimental data on the nature of the solvated electron in THF and the associated wave functions of the electron and sodide to perform such calculations with any accuracy. Our hope is that our quantum molecular dynamics simulations of the sodide/THF system that are currently in progress will allow us to determine the height of the barrier for back electron transfer from the solvated electron to the sodium core.

(61) A detailed examination reveals that the electron appearance time is slightly slower for blue excitation than for red, despite the fact that blue excitation results in a greater average ejection distance. This may result from the fact that a more significant local rearrangement of the solvent is required to produce a solvent-separated contact pair than to produce an immediate contact pair. The extra time for this rearrangement is reflected in the delayed appearance of the electron's equilibrium absorption; cf. Figure 8. In the delayed ejection model, this could be accounted for by assuming (slightly) different detachment rate constants in eqs 5 and 6.

(62) Dye, J. L.; Andrews, C. W.; Ceraso, J. M. *J. Phys. Chem.* **1975**, *79*, 3076. Ceraso, J. M.; Dye, J. L. *J. Chem. Phys.* **1974**, *61*, 1585. Dalton, L. R.; Rynbrandt, J. D.; Hansen, E. M.; Dye, J. L.; *J. Chem. Phys.* **1966**, *44*, 3969.

(63) Similar translational motions into the angular node of a wave function have also been seen in simulation studies of the solvent relaxation following photoexcitation of the hydrated electron. See, e.g.: Schwartz, B. J.; Rossky, P. J. *J. Chem. Phys.* **1994**, *101*, 6902 ref 33.

(64) Peon, J.; Hess, G. C.; Pecourt, J.-M. L.; Yuzawa, T.; Kohler, B. *J. Phys. Chem.* **1999**, *103*, 2460.

(65) Barthel, E. R.; Martini, I. B.; Schwartz, B. J. Manuscript in preparation.

(66) Martini, I. B.; Barthel, E. R.; Schwartz, B. J. *Science* **2001**, *293*, 492.

(67) Kambhampati, P.; Son, D. H.; Kee. T. W.; Barbara, P. F. *Chem. Phys. Lett.* **2001**, *342*, 571.